



## Effect of Aerosols on Visibility and Radiation in Spring 2009 in Tianjin, China

Suqin Han<sup>1</sup>, Hai Bian<sup>1</sup>, Yufen Zhang<sup>2\*</sup>, Jianhui Wu<sup>2</sup>, Yimei Wang<sup>2</sup>, Xuexi Tie<sup>3</sup>, Yinghua Li<sup>1</sup>, Xiangjin Li<sup>1</sup>, Qing Yao<sup>1</sup>

<sup>1</sup> Tianjin Institute of Meteorological Science, Tianjin, 300074, China

<sup>2</sup> State Environmental Protection Key Laboratory of Urban Ambient Air Particulate Matter Pollution Prevention and Control, College of Environmental Science and Engineering, Nankai University, No. 94 Weijin Road, Tianjin 300071, China

<sup>3</sup> National Center for Atmospheric Research, Boulder, CO U.S.A.

---

### ABSTRACT

Meteorological and aerosol data were measured at the atmospheric boundary layer observation station in Tianjin, China, and were analyzed to study the effects of aerosol mass, composition, and size distributions on visibility and short-wave radiation flux. The results show that fine particles played important roles in controlling visibility in Tianjin. The major contributors to light extinction coefficients included sulfate (28.7%), particulate organic matter (27.6%), elemental carbon (19.2%), and nitrate (6.1%). In addition to the measurement of aerosol composition, the size distribution of aerosol number concentrations were also measured and classified between haze days and non-haze days during spring. The extinction characteristics of ambient aerosol in haze days and non-haze days were calculated using Mie theory model. The average extinction coefficient and scattering coefficient of atmospheric aerosols were 0.253 1/km and 0.213 1/km in non-haze days, while 0.767 1/km and 0.665 1/km in haze days. A radiation transmission model LOWTRAN7 is also applied in this study. The model calculated radiant flux densities in haze days and non-haze days, which showed a fairly agreement with the observation results, showing that the heavy aerosol loadings in Tianjin had significantly impact on atmospheric visibility and radiation fluxes.

**Keywords:** Aerosol; Visibility; Extinction coefficient; Refractive index; Radiation fluxes.

---

### INTRODUCTION

With rapid development of urbanization and industrialization, visibility degradation has become an important urban atmospheric environmental problem in Asia (Chan *et al.*, 1999; Bret *et al.*, 2001; Doyle and Dorling, 2002). Visibility was reduced by the scattering and absorption of solar radiation of particles and gaseous pollutants (Latha and Badarinath, 2003). Aerosol plays an important role on atmospheric radiation transmission, though their mass is less than one billion of the total atmospheric mass. In terms of local scale, urban aerosol not only have important effect on extinction of solar radiation, but also affect atmospheric long-wave radiation, which play an important role in local energy balance (Lohmann and Lesins, 2002; Penner *et al.*, 2004; Zhang, 2007; Zhao *et al.*, 2008). Solar radiation reaching the urban ground surface can be

reduced from several to tens percent (Chen *et al.*, 1994). The composition of aerosols has important impact on the calculation of the aerosol radiation effect. For example, element carbon (EC) is a strong absorption aerosol, which had significant influence on visibility, accounting for about 20% of the visibility reduction compared to other aerosol particles (Deng *et al.*, 2008). During the past, many studies focused on the influence of meteorological factors and particle size distribution on atmospheric extinction coefficient and optical depth, while little attention was paid for the effect of aerosol chemical components on visibility (Tian *et al.*, 1996; Chen *et al.*, 2006; Gu *et al.*, 2009). Although the relationships between atmospheric extinction coefficient and aerosol composition is very well know in theory, the study of the impact of aerosol composition on visibility requires measurements of visibility, aerosol mass concentrations, aerosol size distribution, and aerosol composition, which are varied in different regions (Liu and Shao, 2004; Wu, 2008; Wu *et al.*, 2009).

In this paper, the number concentrations with different aerosol bins in haze days and non-haze days during spring were measured by the Grimm instrument. The relationship between visibility and aerosol characteristics (such as aerosol mass concentration, aerosol size distribution, chemical

---

\* Corresponding author. Tel.: 86-22-2350-3397; 1-361-219-2349;  
Fax: 86-022-2350-3397  
E-mail address: zhafox@126.com

composition) was discussed. The Mie theory model was applied to calculate the extinction coefficient of ambient aerosols in haze days and non-haze days. The radiation transmission model (LOWTRAN7) was used for the calculation of radiant flux densities in haze days and non-haze days.

## DATA SOURCES AND TREATMENT

The observation site is located in the atmospheric boundary layer observation station in Tianjin (39°04'N, 117°12'E), which is a residential and traffic mixing area between the Second Ring Road and Outer Ring Road. There is a residential district on the southwest side, a busy Road from the east, and an expressway about 150m from the north. During the experiment period (from Feb 24 to Mar 25, 2009), the number concentration of aerosol, radiant flux densities, and atmospheric visibility were measured by Grimm180 (manufactured by a Germany Company), CNR4 (manufactured by Holand Kipp-zonen Company), and Belfort6000 (manufactured by American Belfort Company), respectively. The real-time online mass concentration of PM<sub>10</sub> and PM<sub>2.5</sub> was measured by RP-1400 particle sampler. Moreover, the vertical distribution of meteorological parameters was measured from the meteorological tower (255 meters) at the observation site and simulation results from a dynamical model (Weather Research and Forecasting, define WRF).

In this paper, haze days were defined as the days when the following weather conditions were occurred, i.e., daily average visibility was less than 10 km and daily average relative humidity was less than 90%, with some special weather days being removed such as precipitation, fly ash, floating dust, smoke and dust storm (Wu *et al.*, 2008). Non-haze days were defined as the days when daily average visibility was more than 10 km. During the observation, there were 18 haze days and 9 non-haze days. The data on Mar 13, Mar 21, and Mar 15 were removed due to the occurrences of light rain, shower, and floating dust, respectively.

In addition, to get the chemical composition of aerosol, PM<sub>10</sub> and PM<sub>2.5</sub> filters sampling were conducted from Mar 9 to Mar 22, 2009. Totally four precalibrated samplers (TH-150, Wuhan Tianhong Intelligence Instrument Facility, China) were installed on the second level of the meteorological tower (10 m above the ground) to collected aerosol samples. PM<sub>10</sub> samples were collected using two samplers, installed impact inlets with nominal aerodynamic cut-off diameter of 10 μm. Among the two samplers, one contained polypropylene filters (90 mm in diameter, Beijing Synthetic Fiber Research Institute, China) for later chemical analysis of inorganic composition in PM<sub>10</sub> samples, and the other quartz-fiber filters (90 mm in diameter, 2500QAT-UP, Pall Life Sciences) for later analysis of organic composition in PM<sub>10</sub> samples. The other two samplers, installed impact inlets with nominal aerodynamic cut-off diameter of 2.5 μm, were used to collect PM<sub>2.5</sub> samples. Similarly, among the two PM<sub>2.5</sub> samplers, one contained polypropylene filters and the other quartz-fiber filters, for later chemical analysis of inorganic composition and organic composition in PM<sub>2.5</sub>, respectively. All samples

were collected at a flow rate of 100 L/min and in a 24-hr period.

Water-soluble inorganic ions were analyzed using the ion chromatography (DX-120, Dionex Ltd., USA) after sample extraction with deionized water (Xue *et al.*, 2010). Organic carbon (OC) and elemental carbon (EC) using the thermal optical carbon analyzer (Desert Research Institute (DRI). Model 2001, Atmoslytic Inc., Calabasas, CA, USA). A 0.5 cm<sup>2</sup> punch of each sample was analyzed for eight carbon fractions following the IMPROVE A protocol (Hou *et al.*, 2011).

## CHARACTERISTICS OF CHANGES IN AEROSOL MASS CONCENTRATION AND VISIBILITY

### *Relationship between Aerosol Mass and Visibility*

Fig. 1 shows the changes in daily average concentration of PM<sub>2.5</sub> and PM<sub>10</sub>. The range of mass concentration of PM<sub>10</sub> and PM<sub>2.5</sub> were between 63–391 and 23–134 μg/m<sup>3</sup> respectively. The corresponding visibility ranged between 3.9 and 20 km, showing that there was a strong anti-correlation between the concentrations of PM and the visibility. In the following sections, the relationship between aerosols (concentrations, size distributions, and composition) and visibility will be analyzed.

Visibility during the observation period was calculated by grading the particle concentration of different size (Table 1). It is found that the average visibility of non-haze day was 16.7 km, while the average visibility of haze day was 5.2 km. To reach the threshold point, at which the reduction of visibility changes from haze day to non-haze day level, the corresponding PM<sub>10</sub> concentrations need to reduce by 47%, and PM<sub>2.5</sub> mass concentration by 67%.

The relationship of particles size and visibility level showed that PM<sub>2.5</sub> accounted for a large proportion in PM<sub>10</sub> (76%) during haze day period (implying that the concentration of fine particles (PM<sub>2.5</sub>) was 3.6 times higher than the coarse particles (PM<sub>2.5–10</sub>)), suggesting that fine particle is a main factor affecting the visibility in Tianjin. This result is consistent with the study by Deng *et al.* (2008) in Guangzhou, China.

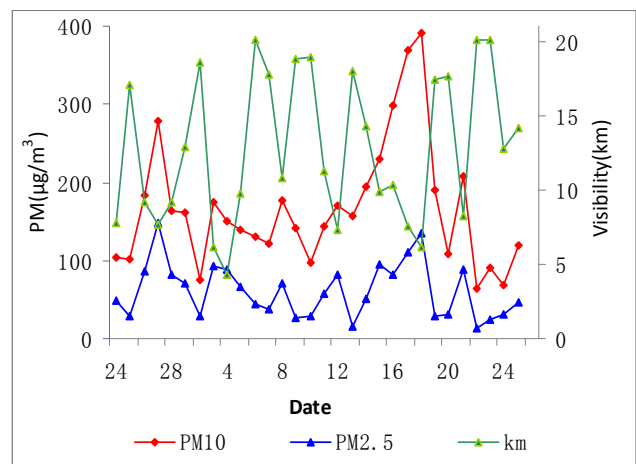


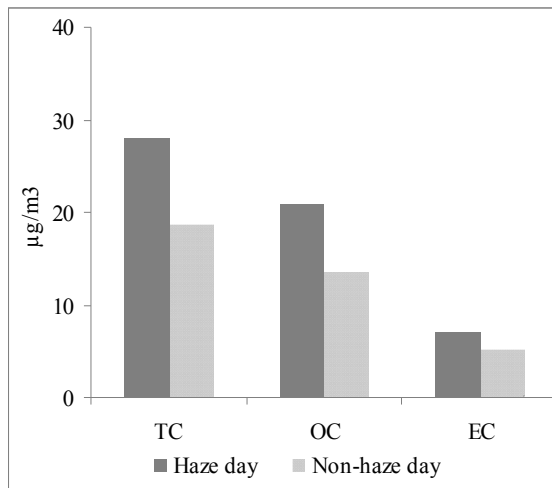
Fig. 1. Variation of aerosol mass concentration and visibility.

**Table 1.** Relationship between visibility grading and particle size.

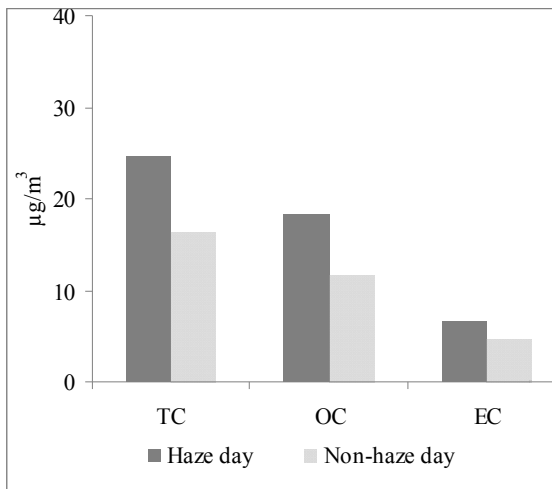
Level	Visibility km	PM <sub>10</sub> µg/m <sup>3</sup>	PM <sub>2.5</sub> µg/m <sup>3</sup>	PM <sub>2.5</sub> /PM <sub>10</sub>	PM <sub>2.5</sub> /PM <sub>2.5-10</sub>
Haze day	5.2	311.2	238.2	0.76	3.6
Non-haze day	16.7	211.8	142.7	0.67	2.07

**Relationship between Aerosol Composition and Visibility**

The individual contribution of different aerosol composition to the reduction of visibility was studied. The total carbon aerosols include elemental carbon and organic carbon. Organic carbon is composed of directed emitted carbon and secondary organic carbon. The measured concentrations of total carbon, elemental carbon, and organic carbon particles were shown in Fig. 2. In non-haze day and haze day, averaged concentrations of total carbon in PM<sub>10</sub> were 18.7 and 28.1 µg/m<sup>3</sup>, respectively. The average concentrations of elemental carbon were 5.1 and 7.1 µg/m<sup>3</sup>, respectively, and the concentrations of organic carbon were 13.6 and 21.0 µg/m<sup>3</sup>, respectively. This result indicated that visibility was inversely correlated with the mass concentration



(a)



(b)

**Fig. 2.** Mass concentration distribution of carbonaceous components in particles in haze days and non-haze days. (a) PM<sub>10</sub>; (b) PM<sub>2.5</sub>.

of carbonaceous particles. During the haze day period, total carbon particles accounted for 9% of total mass of PM<sub>10</sub>. This result suggests that in order to improve the atmospheric visibility level in Tianjin, reduction of carbonaceous aerosol particles is a crucial issue.

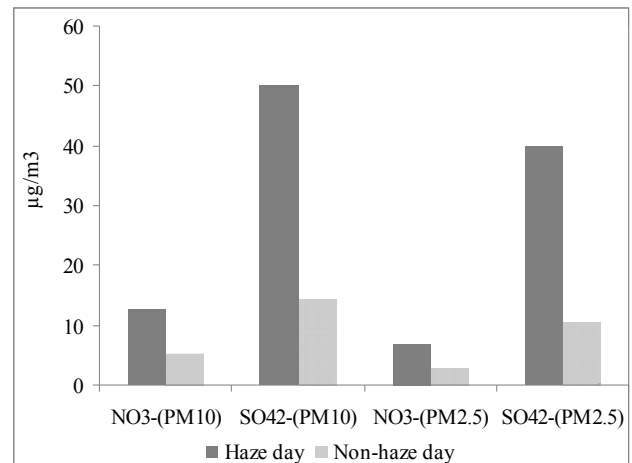
The variations of mass concentration of SO<sub>4</sub><sup>2-</sup> and NO<sub>3</sub><sup>-</sup> under different visibility level were shown in Fig. 3. The result shows that the concentration of SO<sub>4</sub><sup>2-</sup> was considerably higher than NO<sub>3</sub><sup>-</sup>. When the visibility reduced from non-haze day to haze day, both NO<sub>3</sub><sup>-</sup> and SO<sub>4</sub><sup>2-</sup> concentrations increased significantly. The concentrations of SO<sub>4</sub><sup>2-</sup> and NO<sub>3</sub><sup>-</sup> in PM<sub>2.5</sub> increased by 2.8 and 1.4 times, respectively, and the concentrations in PM<sub>10</sub> increased by 2.4 and 1.5 times, respectively. This result shows that both the SO<sub>4</sub><sup>2-</sup> and NO<sub>3</sub><sup>-</sup>, especially SO<sub>4</sub><sup>2-</sup>, have important impacts on the visibility in Tianjin.

Light extinction coefficient from aerosol was calculated by IMPROVE formula (Sisler and Malm, 2000):

$$b_{ext} = 3f(RH)[sulfate] + 3f(RH)[nitrate] + 4[POM] + 10[LAC] + 1[FS] + 0.6[CM] \quad (1)$$

where,  $b_{ext}$  is aerosol extinction coefficient;  $f(RH)$  is relative humidity scattering enhancement factor;  $[sulfate] = 4.125[S]$ ;  $[nitrate] = 1.29[NO_3^-]$ ;  $[particulate\ organic\ matter\ (POM)] = 1.4[OC]$ ;  $[light\ absorbing\ carbon\ (LAC)] = [EC]$ ;  $[fine\ soil\ (FS)] = 2.2[Al] + 2.49[Si] + 1.63[Ca] + 2.42[Fe] + 1.94[Ti]$ ; and  $[coarse\ matter\ (CM)] = [PM_{10}] - [PM_{2.5}]$ .

The average contributions of sulfate, nitrate, particulate organic matter (POM), and elemental carbon (EC) to extinction coefficient were 28.7%, 6.1%, 27.6%, and 19.2%, respectively. Sulfate and particulate organic matter were the major contributors to light extinction coefficient during the observation.

**Fig. 3.** Mass concentration of SO<sub>4</sub><sup>2-</sup> and NO<sub>3</sub><sup>-</sup> in haze days and non-haze days.

## CHARACTERISTICS OF PARTICLE SIZE DISTRIBUTION

The aerosol size distribution indicated that the width of aerosol number density spectrum peaks was narrow, and the corresponding particle size ranged between 0.25 and 0.6  $\mu\text{m}$ . The percentages of particles in the size bins of 0.25–0.28  $\mu\text{m}$ , 0.28–0.30  $\mu\text{m}$ , 0.30–0.35  $\mu\text{m}$ , 0.35–0.40  $\mu\text{m}$ , 0.40–0.45  $\mu\text{m}$ , 0.45–0.5  $\mu\text{m}$  were 27.5, 14.3, 30.8, 13.1, 7.0, and 2.1%, respectively, suggesting that about 98.5% of the total particles were in the radius less than 0.65  $\mu\text{m}$ .

Fig. 4 showed the particle size distribution in haze days and non-haze days. The number density of aerosol in haze days were significantly higher than that in non-haze days, but there was no great difference in the spectrum shape of size distributions between haze days and non-haze days.

Based on the observational data, the aerosol's size distribution in haze and non-haze days were fitted with three-sector-divided Junge & gamma distribution models (Chiara et al., 1997), respectively, as shown in Eqs. (2) and (3), which involved in the calculation of extinction coefficient and scattering coefficients in this study. As the size bin ending at 0.25  $\mu\text{m}$  by GRIMM instrument, the size distribution with diameter less than 0.25  $\mu\text{m}$  was assumed to be the same spectrum model as that in the size bin of 0.25–0.45  $\mu\text{m}$ .

In non-haze days:

$$\frac{dN(r)}{dr} = \begin{cases} 38.0r^{-3.17} & r \leq 0.45 \mu\text{m} \\ 350.0r^{0.3} \exp(-10.0r^{1.0}) & 0.45 < r < 1.0 \mu\text{m} \\ 20.0r^{0.3} \exp(-3.65r^{0.43}) & r \geq 1.0 \mu\text{m} \end{cases} \quad (2)$$

In haze days:

$$\frac{dN(r)}{dr} = \begin{cases} 73.5r^{-3.44} & r \leq 0.45 \mu\text{m} \\ 370.0r^{0.4} \exp(-11.0r^{1.0}) & 0.45 < r < 1.0 \mu\text{m} \\ 20.0r^{0.3} \exp(-3.65r^{0.43}) & r \geq 1.0 \mu\text{m} \end{cases} \quad (3)$$

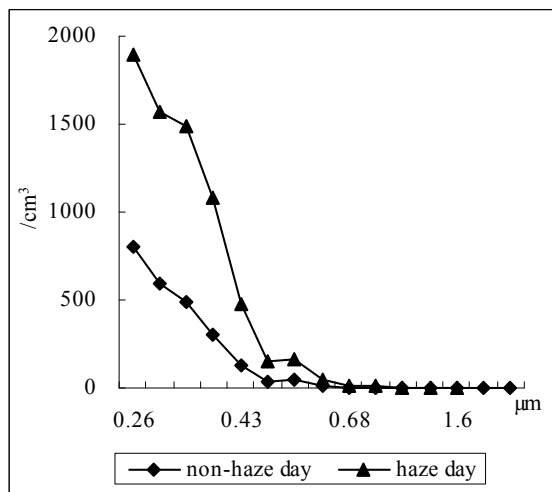


Fig. 4. Distribution of aerosol number density in non-haze days and haze days.

where,  $r$  is the particle size;  $dN(r)/dr$  is number density of aerosol.

## CHARACTERISTICS OF EXTINCTION EFFECTS OF AEROSOL

The Mie theory was used to calculate the scattering coefficient  $b_{sp}$ , extinction coefficient  $b_{ext}$ , and absorption coefficient  $b_{ap}$  as the following equations:

$$\begin{aligned} b_{sp} &= \sum_{i=1}^m b_{sp,i} = \sum_{i=1}^m N_i Q_{s,i} \pi r_i^2 \\ b_{ext} &= \sum_{i=1}^m b_{ext,i} = \sum_{i=1}^m N_i Q_{e,i} \pi r_i^2 \\ b_{ap} &= b_{ext} - b_{sp} \end{aligned} \quad (4)$$

where,  $N_i$  is the number density of  $i$ th particle size interval, described as Eqs. (2) and (3) in this study;  $r_i$  is the median size of  $i$ th particle size interval;  $Q_{s,i}$  and  $Q_{e,i}$  are the scattering and absorption efficiency factors, which are the functions of particle size and refractive index of aerosol given incident wavelength; The particle size measured by GRIMMS is aerodynamic equivalent diameter, while  $r_i$  in Eq. (4) is Stokes diameter. Their transform relationship is as the following:

$$r_i = r_{ca,i} / \sqrt{\rho_i} \quad (5)$$

where,  $r_i$  is the Stokes diameter,  $r_{ca,i}$  is the aerodynamic equivalent diameter, and  $\rho_i$  is the aerosol density of  $i$ th particle size interval.

Refractive index is required for performing radiant calculation and understanding the radiant effect of aerosol. Given chemical components of aerosol, the density  $\rho_i$  refractive index and  $n_i$  of  $i$ th particle size interval can be calculated by the following equation:

$$\begin{aligned} n_i &= \left\{ \sum_j n_j m_j / \rho_j \right\} / \left\{ \sum_j m_j / \rho_j \right\} \\ \rho_i &= \left\{ \sum_j m_j \right\} / \left\{ \sum_j m_j / \rho_j \right\} \end{aligned} \quad (6)$$

where,  $j$  is certain chemical component;  $m_j$  is the mass concentration of  $j$ th component;  $n_j$  is the refractive index of  $j$ th component;  $\rho_j$  is the density of  $j$ th component.

The complex refractive index and density of different chemical component were presented in some literature (Dalzell et al., 1969; Ouimette et al., 1982; Hasan et al., 1983; Sloane, 1983, 1984; Sloane et al., 1985; Sloane, 1986). In this paper, the chemical components considered in later optical calculation are sulfate, nitrate, OC, EC, and other species. Other than sulfate, nitrate, OC, EC, the residual aerosol mass are summarized under "residuals", which is mainly considered as soil dust and/or fly ash for super-1  $\mu\text{m}$  particles. According to the literature (Liu et al., 2004), values of the density  $\rho_j$  and refractive index  $n_j$  of above 5 different

components were listed in Table 2. Based on the measured mass concentration of 5 different chemical compositions  $m_i$  in  $PM_{2.5}$  and  $PM_{10}$  samples, the averaged refractive index for  $PM_{10}$  was  $1.52-0.018i$ , estimated by Eq. (6).

Given above complex refractive index and the number density of aerosol  $N_i$ , as described in formula (2) and (3) in non-haze days and in haze days, the extinction coefficient and scattering coefficients were calculated by integrating the product of number density, the scattering and absorption efficiency factors, and particle size square over particle size from  $0 \mu\text{m}$  to  $10 \mu\text{m}$ , as shown in Eq. (4). In this study, the number of integration points was 100, and the calculated average extinction coefficient and scattering coefficients of aerosol were 0.253 and 0.213  $1/\text{km}$  in non-haze days, while 0.767 and 0.665  $1/\text{km}$  in haze days, respectively.

## NUMERICAL SIMULATION OF THE RADIANT EFFECT OF AEROSOL

### The LOWTRAN7 Model

LOWTRAN7 is an atmospheric radiation transmission model developed by AFGL (Air Force Geophysics Laboratory). In order to calculate the optical characteristics of aerosols, some optical parameters and the LOWTRAN7 model were modified in this study.

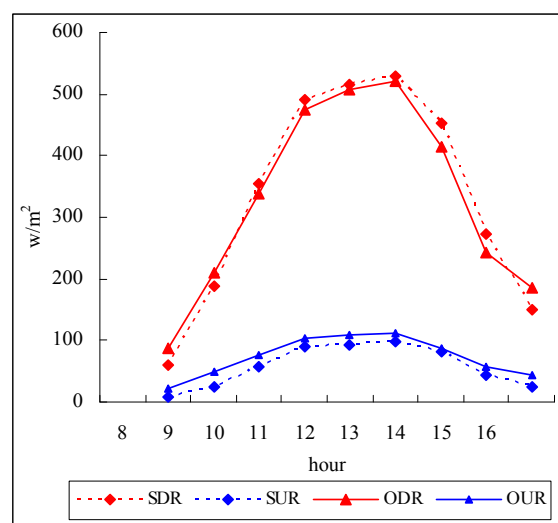
Given the complex refractive index and the number density of aerosol in non-haze days and in haze days during observation in Tianjin, the extinction coefficients and scattering coefficients at 47 wavelength in short-term radiation were calculated by Mie theory and were used to replace the corresponding parameters' database in LOWTRAN7 (Zhang *et al.*, 2006). The numbers of vertical layers in PBL were increased in the modified model, and the height of each layer was 0, 60, 150, 200, 250, 300, 500, 800, and 1000 m, respectively. The profiles of atmospheric temperature, humidity, and pressure below 100 km were modified by the ground meteorological observation data and the simulation results from the WRF model. Detailed information about the WRF model can be found at <http://www.wrf-model.org/index.php>.

### Comparison of Observed and Simulated Radiant Flux Densities

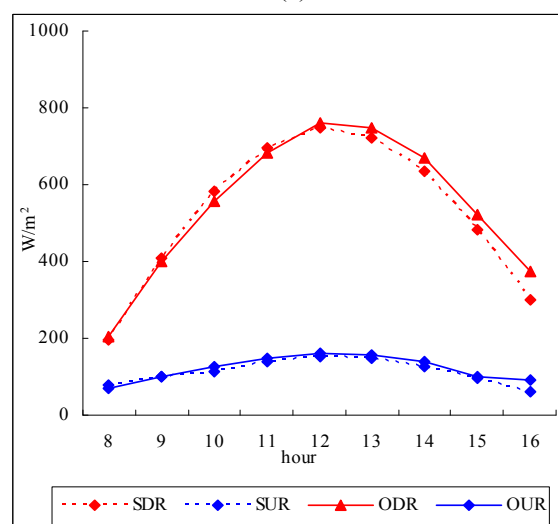
Diurnal variation of ground radiant flux in haze day and non-haze day were simulated using the modified LOWTRAN7 model. Observed and simulated data of radiant flux densities on Mar 3 (haze day) and Mar 6 (non-haze day) were shown in Fig. 5. According to observation of total-and low-cloud covers, almost no any cloud occurred on Mar 3 and 6, except that total cloud amount was 10 at 14:00

**Table 2.** Physical properties of particle composition.

parameters	sulfate	nitrate	EC	OC	residue
density/( $\text{kg}/\text{m}^3$ )	1.76	1.73	2	1.4	2.3
the real part of refractive index	1.52	1.55	1.82	1.45	1.53
the imaginary part of refractive index	0.00015	0.0001	0.47	0.001	0.005



(a)



(b)

**Fig. 5.** Simulated and observed upward (downward) shortwave radiant flux densities. Simulated upward shortwave: SUR; observed upward shortwave: OUR; Simulated downward shortwave: SDR; observed downward shortwave: ODR. (a) On Mar 3, 2009 (haze day); (b) On Mar 6, 2009 (non-haze day).

h on Mar 3. The radiant effects of cloud were simulated by “cloud module” in LOWTRAN7 model. The shortwave radiant flux densities had clearly daily changes, and there was large difference in shortwave radiant flux densities in haze day and non-haze day. The range of simulated and observed downwards short wave radiant flux densities in haze day were 58.7–529.1 and 86.5–520.4  $\text{w}/\text{m}^2$ . The simulated and observed upwards short wave radiant flux densities in haze day ranged from 7.7 to 98.8  $\text{w}/\text{m}^2$ , and from 22.0 to 111.5  $\text{w}/\text{m}^2$ , respectively. While in non-haze day, the simulated downwards and upwards short wave radiant flux densities were in the range of 197.6–746 and 76.9–153.4  $\text{w}/\text{m}^2$ , compared with those observed data in the range of 205.8–762.4 and 67.6–161.6  $\text{w}/\text{m}^2$ , respectively. The simulated shortwave radiant flux densities in haze days

and non-haze days were fairly in agreement with the observed results, which demonstrated that the modified parameters (such as the refractive index, distribution of aerosol number density, and vertical distribution for aerosol's concentration coefficient) comparatively corresponded with the optical characteristics of aerosol in Tianjin during observation.

## CONCLUSION

Characters of visibility variation in Tianjin and its possible influencing factors were analyzed based on meteorological and environmental observation data. Fine particles had greater impacts on visibility than coarse particles in Tianjin; Sulfate and particulate organic matter were the major contributors to light extinction coefficient during the observation. This study suggests that in order to improve the atmospheric visibility levels in Tianjin, particle concentration should be significantly reduced. Moreover, fine sulfate particles and organic carbon should be paid more attentions regarding this environmental concern.

According to the observational data of GRIMMS, the aerosol's size distributions in haze and non-haze days in Tianjin were fitted with a three-sector-divided Junge & Gamma spectrum models, respectively. According to the chemical composition of aerosols over the same period, the extinction characteristics of ambient aerosol were calculated using Mie theory model. It is founded that the average extinction coefficient and scattering coefficient of atmospheric aerosol were 0.253 and 0.213 1/km in non-haze days, while 0.767 and 0.665 1/km in haze days. The LOWTRAN7 model simulated shortwave radiant flux densities in haze days and non-haze days were fairly in agreement with the observation results, which demonstrated that the modified parameters in the model comparatively corresponded with the optical characteristics of aerosol during observation.

## ACKNOWLEDGEMENTS

This work was funded by the public service industrial special research of National Environmental Protection Administration under Grant No.201009001-4 and the Tianjin Municipal Science and Technological Administration under Grant No. 10JCYBJC05800 and 09ZCGYSF02400.

## REFERENCES

- Bret, A.S., Rudolf B.H., Stefan, R.F. and William E.W. (2001). Haze trends over the United States, 1980–1995. *Atmos. Environ.* 35: 5205–5210.
- Chan, Y.C., Simpson, R.W., Mctainsh, G.H., Vowles, P. D., Cohen, D.D. and Bailey, G.M. (1999). Source Apportionment of Visibility Degradation Problems in Brisbane (Australia) Using the Multiple Linear Regression Techniques. *Atmos. Environ.* 33: 3237–3250.
- Chen, C.H., Wang, H.X., Huang, J.G., Zhang, L., Qin, G.Y. and Wang, J.M. (1994). Radiative Effects of Urban Aerosols and their Influence on Mixed Layer Development. *Chin. Sci. Bull.* 39: 56–61.
- Chen, Y.Z., Chai, F.H. and Wei, Q. (2006). Study on Size Distribution of Aerosol Composition in Winter in Beijing. *J. Saf. Environ.* 6: 80–84.
- Chiara, L., Marco, C., Rodolfo G. and Francesca, T. (1997). Atmospheric Aerosol Optical Properties: A Database of Radiative Characteristics for Different Components and Classes. *Appl. Opt.* 36: 8031–8041.
- Dalzell, W.H. and Sarofim, A.F. (1969). Optical Constants of Soot and their Application to Heat-flux Calculations. *J. Heat Transfer* 91: 100–104.
- Deng, X.J., Tie, X., Wu, D., Zhou, X.J., Tan, H.B., Li, F., and Jiang, C. (2008). Long-term Trend of Visibility and its Characterizations in the Pearl River Delta Region (PRD), China. *Atmos. Environ.* 42: 1424–1435.
- Doyle, M. and Dorling, S. (2002). Visibility Trends in the UK 1950–1997. *Atmos. Environ.* 36: 3163–3172.
- Gu, J.X., Bai, Z.P., Xie, Y.Y., Liu, A.X., Wu, L.P. and Sun, M.L. (2009). Characteristics in Light Scattering of Particulate Matter in Tianjin Winter. *Acta. Sci. Nat. Univ. Nankaiensis* 42: 73–86.
- Hasan, H. and Dzubay, T.G. (1983). Apportioning Light Extinction Coefficients to Chemical Species in Atmospheric Aerosol. *Atmos. Environ.* 17: 1573–1581.
- Hou, B., Zhuang, G.S., Zhang, R., Liu, T.N., Guo, Z.G. and Chen, Y. (2011). The Implication of Carbonaceous Aerosol to the Formation of Haze: Revealed from the Characteristics and Sources of OC/EC over a Mega-city in China. *J. Hazard. Mater.* 190: 529–536.
- Latha, K.M. and Badarinath, K.V.S. (2003). Black Carbon Aerosols over Tropical Urban Environment Case Study. *Atmos. Res.* 69: 125–133.
- Liu, X.M. and Shao, M. (2004). The Analysis of Sources of Ambient Light Extinction Coefficient in Summer Time of Beijing City. *Acta. Sci. Circumst.* 24: 186–188.
- Lohmann, U. and Lesins, G. (2002). Stronger Constraints on the Anthropogenic Indirect Aerosol Effect. *Science* 298: 1012–1015.
- Ouimette, J.R. and Flagan, R.C. (1982). The Extinction Coefficient of Multicomponent Aerosols. *Atmos. Environ.* 16: 2405–2419.
- Penner, J.E., Dong, X.Q. and Chen, Y. (2004). Observational Evidence of a Change in Radiative Forcing Due to the Indirect Aerosol Effect. *Nature* 427: 231–234.
- Sisler, J.F. and Malm, W.C. (2000). Interpretation of Trends of PM<sub>2.5</sub> and Reconstructed Visibility from the IMPROVE Network. *J. Air Waste Manage. Assoc.* 50: 775–789.
- Sloane, C.S. (1984). Optical Properties of Aerosols of Mixed Composition. *Atmos. Environ.* 18: 871–878.
- Sloane, C.S. (1983). Optical Properties of Aerosols-Comparison of Measurements with Model Calculations. *Atmos. Environ.* 17: 409–416.
- Sloane, C.S. (1986). Effect of Composition on Aerosol Light Scattering Efficiencies. *Atmos. Environ.* 20: 1025–1037.
- Tian, W.S., Chen, C.H. and Huang, J.G. (1996). Spectral Character and Complex Refractive Index of the Winter Aerosol over Lanzhou City. *J. Lanzhou Univ. (Nat. Sci. Ed.)* 32: 126–132.
- Wu, D. (2008). Discussion on the Distinction between Haze and Fog and Analysis and Processing of Data. *Environ.*

- Chem.* 27: 327–330.
- Wu, D., Mao, J.T., Deng, X.J., Tie, X.X., Zhang, Y.H., Zeng, L.M., Li, F., Tan, H.B., Bi, X.Y., Huang, X.Y., Chen, J. and Deng, T. (2009). Black Carbon aerosols and their Radiative Properties in the Pearl River Delta Region. *Sci. China Ser. D-Earth Sci.* 39: 1542–1553.
- Wu, J., Jiang, W.M., Wang, W.G., Yao, K.Y. and Yuan, R.M. (2004). Simulation of Distribution and Radiative Effects of Dust Aerosol in Spring over China Area. *J. Univ. Sci. Technol. China* 34: 116–125.
- Xue, Y.H., Wu, J.H., Feng, Y.C., Dai, L., Bi, X.H., Li, X., Zhu, T., Tang, X.B., Chen, M.F. (2010). Source Characterization and Apportionment of PM<sub>10</sub> in Panzihua, China. *Aerosol Air Qual. Res.* 10: 367–377.
- Zhang, X.Y. (2007). Aerosol over China and their Climate Effect. *Adv. Earth Sci.* 22: 12–16.
- Zhang, Y.F., Chen, C.H. and Zhu, T. (2006). Study on the Influence of Radiation Effect of Aerosol on PBL Structure. *Abstr. Pap. Am. Chem. Soc.* 231. 137 (Envr): 172–177.
- Zhao, W., Liu, H.N. and Wu, J. (2008). Radiative and Climate Effects of Dust Aerosol on Springs over China. *J. Nanjing Univ. (Nat. Sci.)* 44: 599–607.

*Received for review, May 27, 2011*

*Accepted, October 18, 2011*